Impulse-based Discrete Feedback Control of Motion with Damping Uncertainties

Michael Ruderman and Makoto Iwasaki

Department of Computer Science and Engineering

Nagoya Institute of Technology

Gokiso, Showa, Nagoya, 466-8555, Japan

Email: ruderman.michael@nitech.ac.jp

Abstract—The paper introduces the novel discrete feedback control called here impulse-based. It is believed that the proposed control scheme can be an adequate alternative to other existent robust control methods, like sliding-mode or bang-bang control, when solving the motion control problem with damping uncertainties. The impulse-based control paradigm is introduced while been close related to the well-known impulsive hybrid systems. The stable control convergence is shown for the bounded but unknown positive damping. Also the design of appropriate control parameters is provided in the closed analytic form. Numerical simulation example demonstrates the main control principles and helps to understand its advantages and drawbacks. An experimental case study of the motion control with nonlinear frictional uncertainties in vicinity to position settling discloses the practical relevance of the proposed method.

I. INTRODUCTION

The problem of damping uncertainties belongs to the most relevant in the motion control. While the system inertia can be assumed as well-identifiable and almost time-invariant, the motion damping, in the general sense, is uncertain and can be time- and state-variant to a large extent. In particular, at low relative velocities the motion damping appears as nonlinear and highly irregular for being accurately modeled and identified. As implication, the robust control schemes are often required in the motion control, for instance for accurate tracking and positioning. The motivation behind the recent work is the fact that the linear feedback controls have trouble dealing with the large system uncertainties, on the one hand. On the other hand, the robust feedback controls with discontinues action, like sliding-mode or bang-bang, can be suboptimal in regard to the control norm and system wear.

A novel *impulse-based discrete feedback control*, which appears as close related to the hybrid impulsive systems [1], [2], is introduced. The proposed control action at zero-crossing of state axes can be well-understood when taking a classical example of colliding masses. At impact, the motion velocity undergoes an instantaneous change while no changes are assumed in the position state. The overall system behavior can be then described by impulsive differential equations [1]. Recall that the latter apply the ordinary differential equations at all times except the times of impulses. Therefore, the solutions of corresponding differential equations $\dot{x}(t) = f\big(x(t)\big)$ are piecewise absolutely continuous, while at impulse times t_i the states are governed by some jump map $x(t_i^+) = x(t_i) + c\big(x(t_i)\big)$. Relating to the unified framework, introduced in [3] for the hybrid control, the control scheme proposed here falls into the class of *autonomous-impulse hybrid systems*. This inevitably

leads to the hybrid system consideration (see e.g. books [1], [2]). An extensive and detailed tutorial on the modeling of hybrid systems, their stability theory, and illustrative examples is provided in [4]. It is worth to recall that "the investigation of hybrid systems is creating a new and fascinating discipline bridging the control engineering, mathematics, and computer science" [5]. This is undoubtedly due to the generality of hybrid system methodology which allows dealing with various natural and artificial systems, where the continuous and discrete dynamics coexist and interact with each other. A substantial part of the literature on hybrid systems and hybrid controls has been devoted to stability analysis and stabilization [6]. Former, the perspectives and results on the stability and stabilizability of hybrid systems have been discussed in [7]. Further, the exponential and asymptotic stability of class of hybrid impulsive and switching systems have been studied with a new hybrid control strategy in [6]. The stability analysis of switched systems, which are a particular case of hybrid systems, has been reviewed in [8] while using the variational principles. Here we note that in the recent work, however, the stability analysis of motion system with impulsive behavior is done by means of the phase-plane analysis only, and that due to an obviously simple jump set and jump map of impulsive state transitions. In [9] the impulse control has been analyzed while allowing for control inputs consisting not only of delta functions but equally of their higher derivatives. It has been noted that the norm of impulse controls is lower than that of the bang-bang control and the former are more robust.

Despite the powerful framework and methodology of hybrid control systems their application in several engineering fields remains rather modest than one might expect. This is not least due to the use of quite sophisticated tools from many different fields of applied mathematics, like e.g. applicability of differential inclusions [8]. Also in the motion control, relatively little applications have been demonstrated with use of the impulsive and/or switching hybrid control methods. As one of the few examples, in [10] the authors reported on a hybrid switching control strategy for nonlinear and underactuated mechanical systems evaluated experimentally on the Pendubot.

The recent work is validated by a well-motivating experimental case study of the controlled motion with nonlinear frictional uncertainties (see e.g. [11], [12] for details). Recall that the latter can give rise to the miss of motion target, e.g. positioning, even if a linear feedback regulation is on-going. It is believed that the proposed control scheme can be an adequate alternative to other existing robust control methods.

II.   IMPULSE-BASED DISCRETE CONTROL

We consider the motion system of type

$$\ddot{x}(t) + D\big(\xi(t)\big)\dot{x}(t) = u(t). \tag{1}$$

Note that here and further on a unity inertia (moving mass) is assumed for the sake of simplicity. The unknown disturbance $\xi(t)$ drives the system damping which complies

$$0 < \underline{D} \leqslant D(\xi) \leqslant \overline{D}. \tag{2}$$

The subscript $\underline{D}$ and superscript $\overline{D}$ indicate the corresponding boundaries. For an arbitrary initial state $(x_0, \dot{x}_0)$ at time t_0, the free motion of (1) results in trajectories as depicted in Fig. 1. Note that we consider a relative motion starting in
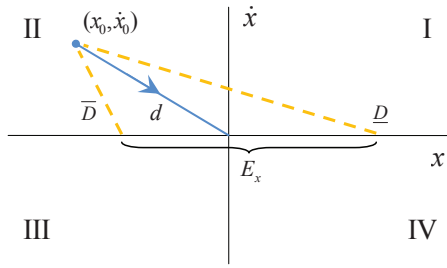

Fig. 1.   Free motion trajectories of system (1) with damping uncertainties

the II-nd quadrant, while due to the symmetry an equivalent consideration of initial states in the IV-th quadrant can be done. Further, one can recognize that for $D(\xi) = \text{const} = d$ the trajectory of system (1) converges to zero equilibrium which we are interested in. Here it should be noted that the systems of type $\ddot{x}(t) + d\dot{x}(t) = 0$ can already incorporate an appropriate linear feedback control which guarantees the reachability of zero equilibrium, provided no damping uncertainties are present. However, the assumed $D(\xi)$ leads to an under- or otherwise over-damped motion that results in a trajectory manifold. The latter yields an infinite set of possible equilibria E_x as schematically shown in Fig. 1.

Proposition 1:

Apply the following discrete feedback control

$$u(t) = -\lambda_x \frac{\mathrm{d}}{\mathrm{d}t}\text{sign}\big(x(t)\big) - \lambda_{\dot{x}} \text{sign}\big(x(t)\big)\Big|\frac{\mathrm{d}}{\mathrm{d}t}\text{sign}\big(\dot{x}(t)\big)\Big|, \tag{3}$$

where $\lambda_x > 0$ and $\lambda_{\dot{x}} > 0$ are the design parameters. Analyzing (3) one can recognize that the control action occurs each time the trajectory crosses one of the $[x, \dot{x}]$-axes. Note that the corresponding control effort constitutes the double Dirac impulse which is weighted by the factors λ_x and $\lambda_{\dot{x}}$ respectively. Due to orthogonality of the $(x, \dot{x})$ space both control parts are disjunct and act simultaneously in $(0,0)$ only, where the overall control action is zero, according to (3). Therefore, both right-hand side terms of (3), denoted in the following as control (i) and (ii) respectively, can be analyzed separately, while they have been joint by the logical operator 'or'.

(i) position zero-crossing control

Substituting the first right-hand side term of (3) into (1) results in the control system dynamics

$$\ddot{x}(t) + D\dot{x}(t) = -\lambda_x \frac{\mathrm{d}}{\mathrm{d}t}\text{sign}\big(x(t)\big). \tag{4}$$

Note that for the sake of simplicity here and further on we write the damping term D without ξ argument. Integrating (4) with respect to the time one obtains

$$\dot{x}(t) = -Dx(t) - \lambda_x \text{sign}\big(x(t)\big). \tag{5}$$

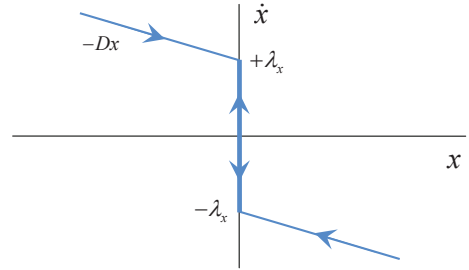The corresponding trajectories are depicted in Fig. 2. Important

Fig. 2.   Trajectory of system (4) with discrete control law (i)

to note is that once the trajectory attains $x = 0$ it belongs to the set of $\dot{x}$ values lying between $\pm\lambda_x$. However, since real physical systems possess finite acceleration values, the real trajectories will slightly deviate from the $\dot{x}$-axis, and that by some small Δx value depending on the actuator constraints and control sample time. The trajectory will transform into inclined cyclic orbits as schematically shown in Fig. 3. Note
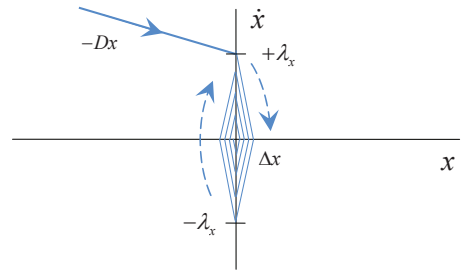

Fig. 3.   Inclined cyclic orbits around $x = 0$ state

that the cyclic orbits converge slowly towards zero equilibrium, since the motion system is positively damped.

Proposition 2:

Let the control parameter λ_x be

$$\lambda_x = \alpha\big|\dot{x}(t_{x0})\big| \quad \text{with} \quad 0.5 < \alpha < 1, \tag{6}$$

where t_{x0} is the time instant of trajectory crossing the $\dot{x}$-axis, i.e. the time instant of discrete control action $\mathrm{d}/\mathrm{d}t\,\text{sign}(x)$. We are to show that for any zero crossing state $(0, \dot{x}_{x0})$ the control parameter (6) leads to the stable system convergence, and the convergence rate is controlled by the α-parameter selection.

Since zero-crossing control action constitutes the weighted (by λ_x) double Dirac impulse 2δ, with

$$\int \delta(t)dt = 1,$$

the system (4) can be rewritten as

$$\ddot{x}(t) + D\dot{x}(t) = -2\lambda_x \delta(t), \qquad (7)$$

and transformed into the Laplace s-domain as

$$x(s)s^2 + Dx(s)s = -2\lambda_x. \qquad (8)$$

Note that the sign on the right-hand side of (7), and correspondingly (8), depends on the sign of instantaneous velocity at t_{x0}. This, however, does not influence the generality of analysis we perform below. Transforming back the $x(s)$ solution of (8) into the time domain one obtains

$$x(t) = -\frac{2\lambda_x}{D}\left(1 - e^{-Dt}\right), \qquad (9)$$

and correspondingly

$$\dot{x}(t) = -2\lambda_x e^{-Dt}. \qquad (10)$$

Combining the general velocity solution (10) of system (7) with the particular solution of the free motion with an initial state $(0, \dot{x}_{x0})$ one obtains

$$\dot{x}(t) = \left(-2\lambda_x + \dot{x}_{x0}\right) e^{-Dt}. \qquad (11)$$

Further, we are interested in considering the time instant $t = 0^+$, that is immediately after the position zero-crossing. Substituting (6) into (11) results in

$$\dot{x}(0^+) = \lim_{t\to 0^+} \left(-2\alpha|\dot{x}_{x0}| + \dot{x}_{x0}\right) e^{-Dt} = -2\alpha|\dot{x}_{x0}| + \dot{x}_{x0}. \qquad (12)$$

It can be seen that when selecting α according to (6), the trajectory will jump after the velocity zero-crossing into the opposite direction while attaining the velocity magnitude

$$0 < \left|\dot{x}(0^+)\right| < |\dot{x}_{x0}|,$$

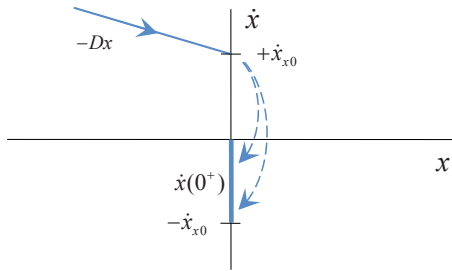as schematically illustrated in Fig. 4. The described above

Fig. 4.   Velocity transitions at the control parameter (6)

impulsive system behavior repeats with a decreasing velocity magnitude each time the position sign changes. Therefore, the stable convergence of control system (4), (6) can be ensured.

Remark: Most important is that the described above control behavior does not depend on damping uncertainties, provided the free motion of system (4) is positively damped.

(ii) velocity zero-crossing control

Substituting the second right-hand side term of (3) into (1) results in the control system dynamics for which the following control actions should be diversified

$$u(t) = \begin{cases} -2\lambda_{\dot{x}}\delta(t) & \text{if } x > 0 \ \wedge \ \mathrm{d}/\mathrm{d}t\,\mathrm{sign}\big(\dot{x}(t)\big) \neq 0, \\ 2\lambda_{\dot{x}}\delta(t) & \text{if } x < 0 \ \wedge \ \mathrm{d}/\mathrm{d}t\,\mathrm{sign}\big(\dot{x}(t)\big) \neq 0, \\ 0 & \text{otherwise.} \end{cases} \qquad (13)$$

For the sake of simplicity we denote the above case differentiation sequentially by (a), (b), and (c). Note that $\left|\mathrm{d}/\mathrm{d}t\,\mathrm{sign}\big(\dot{x}(t)\big)\right| = \delta$, i.e. the motion fully stops after a positive or negative velocity, constitutes a special case of (a) and (b) and has a single impact on the $\lambda_{\dot{x}}$ selection. Integrating, with respect to the time, the motion dynamics (1), for which the right-hand side is substituted by (13), results in

$$\dot{x}(t) = \begin{cases} -Dx(t) - 2\lambda_{\dot{x}} & \text{for case (a),} \\ -Dx(t) + 2\lambda_{\dot{x}} & \text{for case (b),} \\ -Dx(t) & \text{for case (c).} \end{cases} \qquad (14)$$

Analyzing (14) one can see that this constitutes a set of possible trajectories as schematically shown in Fig. 5. It is obvious
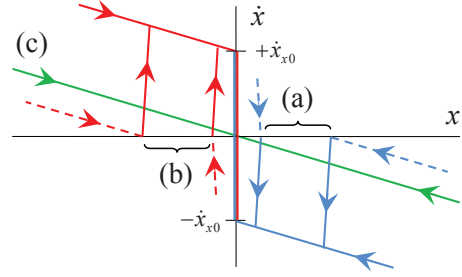

Fig. 5.   Possible motion trajectories after velocity zero crossing

that independent of the run-in initial trajectory the discrete control system (ii) will enforce the relative motion towards $\dot{x}$-axis – the case that we are interested in. Recall that once the trajectory attains an arbitrary $(0, \dot{x}_{x0})$ state the control (i) will provide a stable convergence to zero equilibrium. Further, it is evident that higher values of control parameter $\lambda_{\dot{x}}$ lead to the trajectory attending faster the $\dot{x}$-axis, on the one hand. On the other hand, the control (ii) can by-effect the trajectory convergence around the $\dot{x}$-axis when the velocity sign changes and consequently the control (ii) co-acts. Apart from that, the too large $\lambda_{\dot{x}}$ values can lead to the unnecessarily high velocities when reaching the $\dot{x}$-axis and, as a consequence, to unnecessary action of the control (i).

Proposition 3:

Let the control parameter $\lambda_{\dot{x}}$ be

$$\lambda_{\dot{x}} = \beta\left|x(t_{\dot{x}0})\right| \quad \text{with} \quad \beta > \frac{\overline{D}}{2}, \qquad (15)$$

where $t_{\dot{x}0}$ is the time instant of trajectory crossing the x-axis. Having the general solution

$$\dot{x}(t) = \pm 2\lambda_{\dot{x}} e^{-Dt} \qquad (16)$$

of the relative velocity at nonzero control action (13) and a free motion afterwards, which is described by

$$\dot{x}(t) = -Dx(t),$$

one can see that the displacement range until the relative motion stops again is

$$|x^*| = \frac{2\lambda_{\dot{x}}}{D}.$$

It is evident that in order to enforce the trajectory for reaching the $\dot{x}$-axis from any initial position $x_{\dot{x}0}$, and that possibly with one discrete control action only, the following condition should be fulfilled

$$\frac{2\lambda_{\dot{x}}}{D} \geq |x_{\dot{x}0}|. \tag{17}$$

That leads to the control parameter as proposed in (15) when taking into account the damping uncertainties.

Now let us analyze the by-effect of control (ii) in vicinity to $\dot{x}$-axis, as mentioned before the Proposition 3. With respect to the control (13) and (15) the instantaneous velocity (12) after zero-crossing becomes

$$\dot{x}(0^+) = -2\alpha|\dot{x}_{x0}| - 2\beta|x_{\dot{x}0}| + \dot{x}_{x0}. \tag{18}$$

It is evident that since $|x_{\dot{x}0}| \to 0$ no real impact on the convergence of control (i) appears owing to the by-effect of control (ii). However, due to the finite sampling rates of control implementation it is suggested to reinforce the parameter boundaries (6) by selecting $0.6 < \alpha < 0.9$.

III. NUMERICAL EXAMPLE

The following numerical example illustrates the principal behavior of the proposed impulse-based discrete feedback control. The motion system (1) is simulated with the time-varying damping $D(t)$ as depicted in Fig. 6 (a). An initial state $[x, \dot{x}](t_0) = [-0.3, 20]$ is assumed. The control parameter α is selected to be once 0.9 and once 0.6. The control parameter β is set to 20 (according to (15)) and that in both cases, since this is less relevant for motion convergence. The sampling rate of the performed numerical simulation is 10 kHz.

The resulted position and velocity response are shown in Fig. 6 (b) and (c) correspondingly. The control action of the impulse-based discrete feedback control is depicted in Fig. 6 (d). One can easily recognize that at impulsive control actions the relative velocity changes stepwise and does not depend on damping variations. According to the control law (6) the transient velocity converges to zero depending on the α parameter selection. Obviously, less control impulses are required for lower α values. At the same time, one can see that the control parameter selection does not influence the steady-state accuracy. Further, it is evident that here, the visible control impulses result mainly from the control action (i). It should be noted, however, that when either the α parameter is selected too small or the system uncertainties are too large, in particular owing to the input gain or unknown disturbances, the excited (by control (i)) motion can stop too early. In that case, the control (ii) will enforce the system towards position zero-crossing, respectively zero equilibrium.
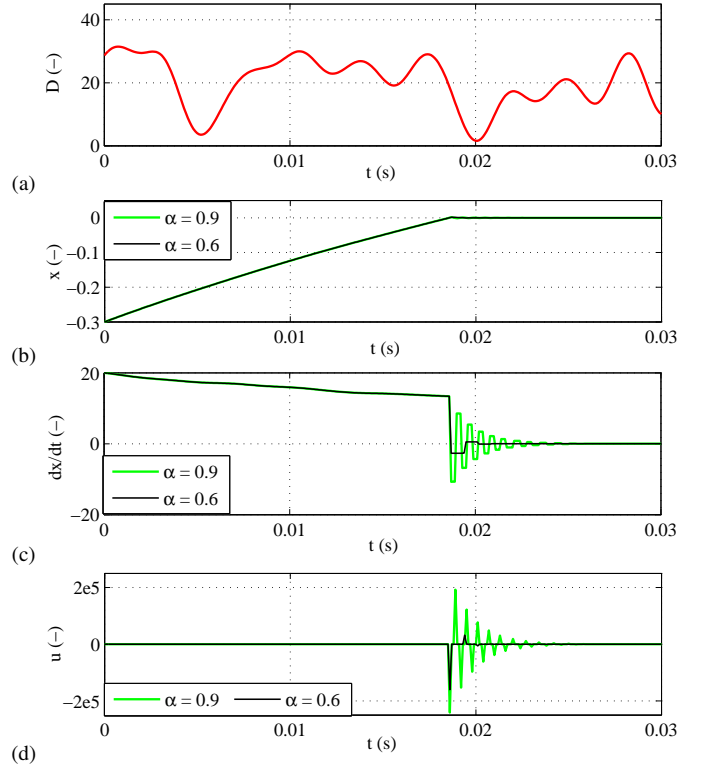

Fig. 6. Simulated response of impulse-based discrete control, (a) time-variant plant damping, (b) position, (c) relative velocity, (d) control action

IV. EXPERIMENTAL CASE STUDY

The experimental case study has been carried out on a standard industrial linear axis actuated by the BLDC motor (see Fig. 7). The problem of an accurate positioning in presence of
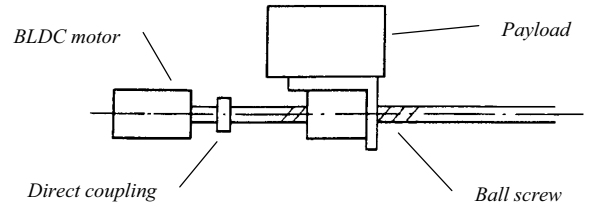

Fig. 7. Experimental setup of actuated linear axis

nonlinear friction and the drawbacks of standard P-PI and PI-PI feedback regulation have been recently studied in details in [13]. Further we recall that the nonlinear friction in the motion control can be efficiently compensated by explicit observer-based methods (see e.g. [14]). However, the latter requires a more elaborated friction modeling and identification, and is out of scope in this work.

In the following, we briefly review the edge characteristics of the motion system, which are most relevant for the control evaluation. The sample time of the digital control unit is 500 μs. The theoretical resolution of linear motion, related to the motor encoder, is 0.3 μm. However, the repeatability of the controlled motion is limited by the backlash in the ball-screw which nominal value accounts for 20 μm. It is evident that the motor-side motion control cannot resolve the steady-state

accuracy beyond this limit. Furthermore, it should be noted that at various load positions, this relating to the load distance to the motor coupling, the disturbing oscillating modes can occur to the varying extent. The latter are due to the axial and torsional stiffness of the ball-screw shaft. Recall that the oscillating modes are not captured by (1) at all, and therefore constitute an additional severity for the control robustness.

A. Nominal linear model

The nominal linear system model

$$\ddot{x}(t) + 22.15\,\dot{x}(t) = 2.077\mathrm{e}4\,u(t)$$

is determined from the measured frequency response function (FRF) depicted in Fig. 8 together with the model response. The FRF has been obtained by applying the random binary signal excitation in the frequency range $0.01 - 50$ Hz and measuring the relative velocity of the motor drive.
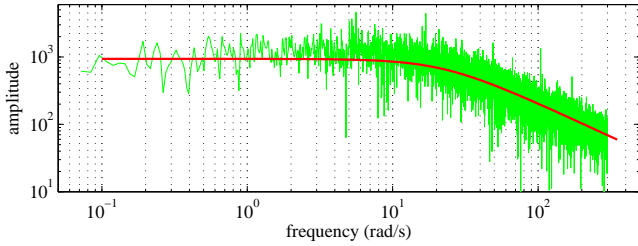

Fig. 8. Measured (grey) and identified (black) frequency response function

B. Free motion with damping uncertainties

The free motion of linear axis is realized by first forcing the system to the steady-state velocity 50 mm/s, and that using the PI feedback velocity control. Afterwards the control input is switched-off at the fixed time instant t_{off}. Note that at t_{off}^{+} the time counter (clock) is reset to zero and the relative position value is set to $x(t_{\mathrm{off}}^{+}) = -0.6$ mm. The latter is further used as an initial position during the control evaluation described in Section IV-C.
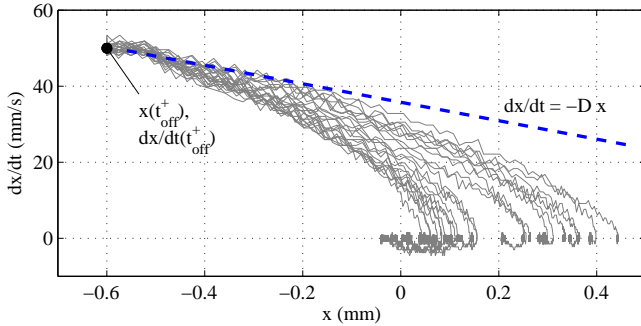

Fig. 9. Measured free motion trajectories with damping uncertainties

The trajectories manifold recorded from the multiple experiments is shown in Fig. 9. Note that while the initial velocities $\dot{x}(t_{\mathrm{off}}^{+})$ are relatively close to each other, the initial positions of the controlled drive $x(t_0)$ have been chosen arbitrary. Therefore $x(t_{\mathrm{off}}^{+})$ corresponds to the different load

positions along the ball-screw shaft. The measured free motion trajectories disclose a wide spread of the final equilibria and, furthermore, significantly differ from the nominal $\dot{x} = -D\,x$ trajectory, which is indicated in Fig. 9 as well. Further it can be noted that the secondary resonant mode, as mentioned in Section IV-A, becomes remarkable in vicinity to the position settling.

C. Control evaluation

The impulse-based discrete feedback control, implemented according to Section II, has been experimentally evaluated to attend zero position equilibrium. Once the initial position has been set to $x(t_{\mathrm{off}}^{+}) = -0.6$ mm, as mentioned before in Section IV-B, and once to $x(t_{\mathrm{off}}^{+}) = -0.2$ mm. Note that the average velocity of free motion at the first zero-crossing of $\dot{x}$-axis is about 15 mm/s in the first case and about 45 mm/s in the second case. The selected control parameters are $\alpha = 0.65$ and $\beta = 20$. Note that the discrete-time approximated Dirac impulses are modulated into the corresponding pulses, and that with regard to the actuator constraints, i.e. $|u_{\max}| = 1.5$ Nm. The energy content of the modulated pulses equal, however, to that of the corresponding impulses.
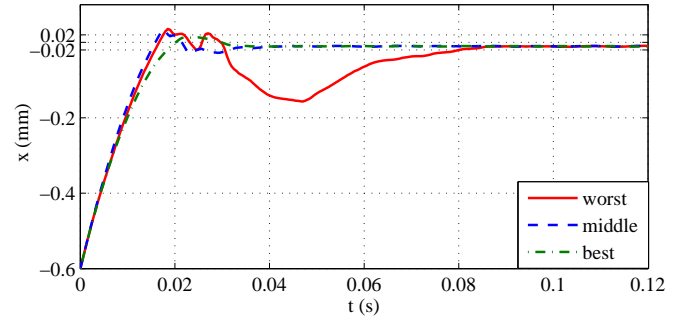

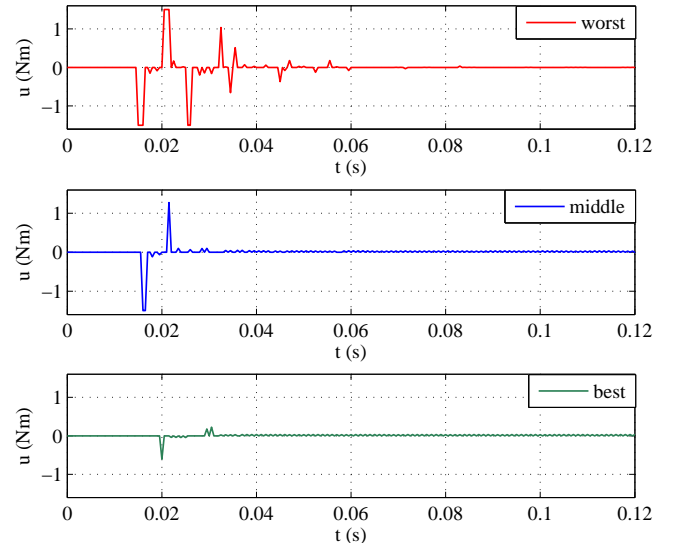Fig. 10. Measured response of the controlled position at 0.6 mm distance

Fig. 11. Measured control effort at 0.6 mm distance

Numerous control experiments have been repeated independently, from which those with the 'worst', 'middle', and

'best' performance are shown in Fig. 10 for the 0.6 mm positioning distance. Note that both, settling time and oscillating behavior around zero position, have been considered as control performance. Recall that the steady-state error band, indicated in Fig. 10, is due to the backlash in the positioning system. In all cases, the control attains zero equilibrium. Inspecting the corresponding control efforts in Fig. 11 one can recognize that in the 'best' case two consecutive impulses are sufficient for the position convergence. In the 'worst' case, a sequence of decreasing impulses equally drives the system to zero equilibrium. It should be noted that the minor steady-state control oscillations can occur as impact of the backlash.
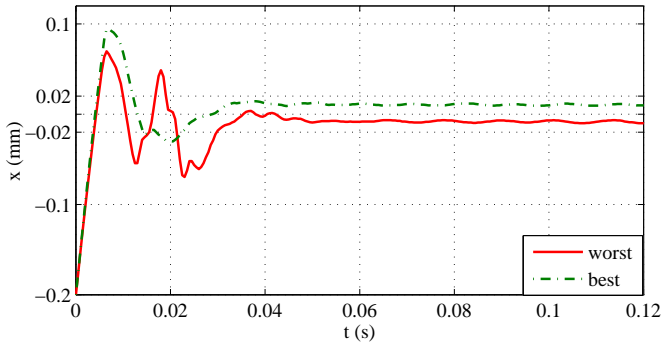

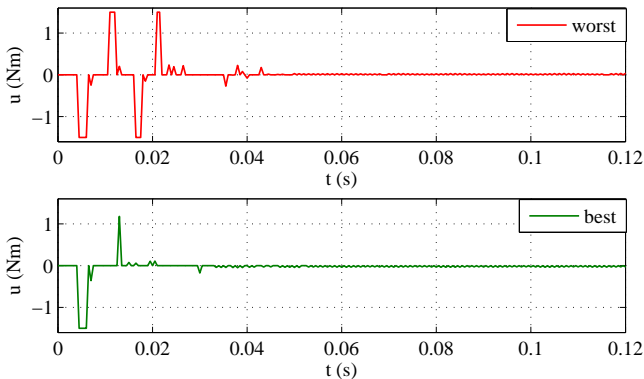Fig. 12. Measured response of the controlled position at 0.2 mm distance

Fig. 13. Measured control effort at 0.2 mm distance

The 'worst' and 'best' cases of the positioning on 0.2 mm distance are shown in Figs. 12 and 13. Also here the control enforces the motion system towards zero position equilibrium. The larger first control impulse indicates clearly that the motion should be decelerated starting from the larger zero-crossing velocities than in the case of positioning on the 0.6 mm distance (cf. Figs. 11 and 13).

V. SUMMARY AND OUTLOOK

In this paper, a novel impulse-based discrete feedback control has been proposed which is closely related to impulsive hybrid systems. While the overall behavior and stability of the control system have been investigated using the phase-plane analysis, this mainly due to the relatively trivial jump set and jump map, its formulation clearly falls into the class of autonomous-impulse hybrid systems. This allows properly applying the impulsive differential equations, or more generally

differential inclusions, in order to perform future investigations towards more complex motion dynamics.

The proposed control scheme is quite simple and, at the same time, offers several advantages comparing to other robust control schemes like bang-bang or sliding-mode control. Amongst, the control norm, i.e. power consumption, seems to be lower, the plant is less subject to the wear, and the required a-priory plant knowledge appears to be marginal. Another important feature is that the proposed control scheme can be easily integrated as an additional plug-in compensator, without the need of redesigning the surrounding feedback control loop. One well-motivating experimental case study of motion control with a large impact of friction nonlinearities at low velocities has demonstrated the efficiency of the proposed method.

For further investigations, several implementation-related issues appear as significant, these apart from the underlying theoretical analysis of hybrid impulsive behavior. On the one hand, the impact of sensor noise should be analyzed while been related to the used zero-crossing detection. On the other hand, the modulation of Dirac impulses, which is required under the actuator constraints, should be studied. The latter directly affects the corresponding jump map and can have a significant impact on the overall control behavior.

REFERENCES

[1] T. Yang, *Impulsive control theory*. Berlin: Springer, 2001.

[2] B. Miller and E. Rubinovich, *Impulsive Control in Continuous and Discrete-Continuous Systems*. New-York: Springer US, 2003.

[3] M. Branicky, V. Borkar, and S. Mitter, "A unified framework for hybrid control: model and optimal control theory," *IEEE Transactions on Automatic Control*, vol. 43, no. 1, pp. 31–45, 1998.

[4] R. Goebel, R. Sanfelice, and A. Teel, "Hybrid dynamical systems," *IEEE Control Systems Magazine*, vol. 29, no. 2, pp. 28–93, 2009.

[5] P. Antsaklis, "Special issue on hybrid systems: theory and applications a brief introduction to the theory and applications of hybrid systems," *Proceedings of the IEEE*, vol. 88, no. 7, pp. 879–887, 2000.

[6] Z.-H. Guan, D. Hill, and X. Shen, "On hybrid impulsive and switching systems and application to nonlinear control," *IEEE Transactions on Automatic Control*, vol. 50, no. 7, pp. 1058–1062, 2005.

[7] R. DeCarlo, M. Branicky, S. Pettersson, and B. Lennartson, "Perspectives and results on the stability and stabilizability of hybrid systems," *Proceedings of the IEEE*, vol. 88, no. 7, pp. 1069–1082, 2000.

[8] M. Margaliot, "Stability analysis of switched systems using variational principles: An introduction," *Automatica*, vol. 42, no. 12, pp. 2059–2077, 2006.

[9] A. Daryin and A. Kurzhanski, "Impulse control inputs and the theory of fast feedback control," in *IFAC World Congress*, 2008, pp. 4869–4874.

[10] M. Zhang and T. Tarn, "A hybrid switching control strategy for nonlinear and underactuated mechanical systems," *IEEE Transactions on Automatic Control*, vol. 48, no. 10, pp. 1777–1782, 2003.

[11] F. Al-Bender and J. Swevers, "Characterization of friction force dynamics," *IEEE Control Systems Magazine*, vol. 28, no. 6, pp. 64–81, Dec. 2008.

[12] M. Ruderman and T. Bertram, "Two-state dynamic friction model with elasto-plasticity," *Mechanical Systems and Signal Processing*, vol. 39, no. 1–2, pp. 316–332, 2013.

[13] M. Ruderman and M. Iwasaki, "Analysis of settling behavior and design of cascaded precise positioning control in presence of nonlinear friction," in *IEEE International Power Electronics Conference*, 2014, pp. 1665–1670.

[14] M. Ruderman, "Tracking control of motor drives using feed-forward friction observer (FFFO)," *IEEE Transactions on Industrial Electronics*, vol. 61, no. 7, pp. 3727–3735, 2014.